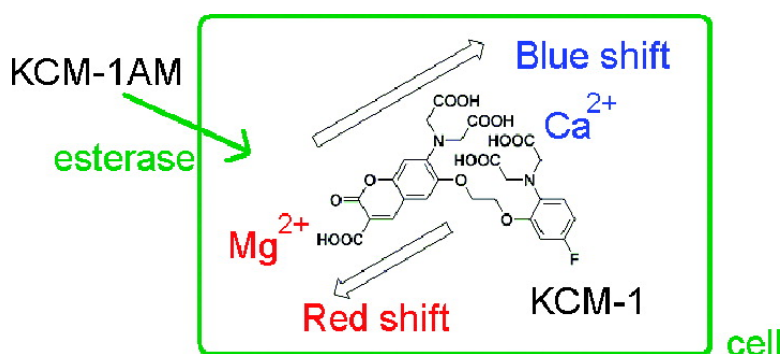


Single Molecular Multianalyte (Ca, Mg) Fluorescent Probe and Applications to Bioimaging

Hirokazu Komatsu, Takahiro Miki, Daniel Citterio, Takeshi Kubota, Yutaka Shindo, Yoshiichiro Kitamura, Kotaro Oka, and Koji Suzuki

J. Am. Chem. Soc., **2005**, 127 (31), 10798-10799 • DOI: 10.1021/ja0528228 • Publication Date (Web): 14 July 2005

Downloaded from <http://pubs.acs.org> on March 25, 2009



More About This Article

Additional resources and features associated with this article are available within the HTML version:

- Supporting Information
- Links to the 12 articles that cite this article, as of the time of this article download
- Access to high resolution figures
- Links to articles and content related to this article
- Copyright permission to reproduce figures and/or text from this article

[View the Full Text HTML](#)

Single Molecular Multianalyte (Ca²⁺, Mg²⁺) Fluorescent Probe and Applications to Bioimaging

Hirokazu Komatsu, Takahiro Miki, Daniel Citterio, Takeshi Kubota, Yutaka Shindo, Yoshiichiro Kitamura, Kotaro Oka, and Koji Suzuki*

Departments of Applied Chemistry and of Bioscience and Informatics, Faculty of Science and Technology, Keio University, 3-14-1 Hiyoshi, Kohoku-ku, Yokohama, Kanagawa 223-8522, Japan

Received April 30, 2005; E-mail: suzuki@applc.keio.ac.jp

Fluorescent imaging based on fluorescent probes offers a highly sensitive, high-speed spatial and temporal analysis of cells¹ and is widely used in the field of biology and physiology. The development of excellent fluorescent probes is required for better fluorescent imaging, thus highly selective fluorescent probes have already been developed, including fura-2² and fluo-3³ for Ca²⁺, KMG-20⁴ and 104⁵ for Mg²⁺, DAFs⁶ for NO, etc. With these molecular fluorescent probes, selective imaging of a particular analyte has been investigated. Since intracellular signal transduction results from various signal transmitters, the simultaneous monitoring of multiple analytes has been attempted with simultaneous loading of several indicators in a cell.⁷ However, the combination of several indicators produces cross-talk, a larger invasive effect, and the different localization, metabolisms, and photobleaching rates of individual indicators make the situation complicated and unsuitable for quantitative analysis.

In this study, we demonstrate that the use of a single-molecular multianalyte sensor, namely, a single probe that allows the sensing of multiple analytes with different spectral responses, is a promising way to overcome the difficulties encountered when loading multiple indicators.

Ca²⁺ is the intracellular divalent cation with the largest concentration variations and plays a critical role as a signal transmitter,⁸ while Mg²⁺ is the most abundant divalent cation and acts as a cofactor in many situations.⁹ However, the correlation of the Ca²⁺ and Mg²⁺ concentrations is not clear and has sometimes been reported to behave proportionally¹⁰ and at other times inverse proportionally.¹¹ Thus, to clarify the situation, a highly sensitive spatially and temporally resolved monitoring of both cations is required.

We now report on the simultaneous imaging of intracellular Ca²⁺ and Mg²⁺ with a novel single-molecular multianalyte sensor, the Ca²⁺–Mg²⁺ multifluorescent probe.

We designed the first Ca²⁺–Mg²⁺ multifluorescent probe, KCM-1, by combining in a single molecule a coumarin moiety as a stable fluorophore⁴ excitable with visible light, BAPTA (*O,O'*-bis(2-aminophenyl)ethyleneglycol-*N,N,N',N'*-tetraacetic acid) as the Ca²⁺ selective binding site^{1–3,12} at the electron-donor site of the chromophore, and a charged β -diketone as the Mg²⁺ selective binding site^{4,5} at the electron-accepting site. The dissociation constants of the BAPTA derivative are typically on the order of 0.1–1 μ M for Ca²⁺ and 1 mM for Mg²⁺, while those of the charged β -diketone are on the order of 10 mM for Ca²⁺ and 1–10 mM for Mg²⁺. A fluorine-substituted BAPTA¹³ was chosen as the Ca²⁺ selective binding site due to its low Mg²⁺ affinity. In the event of Ca²⁺ binding to BAPTA, the cation binding to the electron-donor site of the chromophore leads to a blue shift in the absorbance and fluorescence spectra based on an ICT-type mechanism.¹⁴ On the contrary, Mg²⁺ binding to the β -diketone electron-acceptor site induces a red shift of the spectral bands.

KCM-1 was successfully synthesized starting from the reported fluorine-substituted BAPTA derivative^{13b} (details in Supporting Information).

Figure 1 shows the absorbance and fluorescence spectra of KCM-1 under simulated biological conditions (pH 7.20, 50 mM HEPES, 130 mM KCl, 20 mM NaCl) for different Ca²⁺ or Mg²⁺ concentrations. Upon complexation to Ca²⁺, KCM-1 shows a 45 nm blue shift in absorbance and a 5 nm blue shift in the fluorescence spectrum. For Mg²⁺, a 21 nm red shift in absorbance and a 5 nm red shift in fluorescence occurred.

The binding characteristics of fluorescent probes are often compared based on their dissociation constant, K_d . The dissociation constants of KCM-1 with Ca²⁺ or Mg²⁺ were calculated using the double logarithm plot method² and found to be $14 \pm 1 \mu$ M in the case of $K_d(\text{Ca}^{2+})$ and $26 \pm 3 \text{ mM}$ for $K_d(\text{Mg}^{2+})$. While the intracellular Ca²⁺ concentration is on the order of 0.1–1 μ M and the Mg²⁺ concentration is 1 mM, the experimentally determined dissociation constants indicate relatively low affinities. However, low-affinity indicators are reported to be useful for quantification of high concentrations and of transient responses.¹⁵ The basic optical properties and the dissociation constants are summarized in Table 1 and are consistent with the molecular design strategy.

To investigate the performance of KCM-1 in the simultaneous presence of Ca²⁺ and Mg²⁺, the absorbance and fluorescence spectra of the probe were measured under simulated biological conditions (pH 7.20, 50 mM HEPES, 130 mM KCl, 20 mM NaCl) with different mixed Ca²⁺ and Mg²⁺ concentrations.

On the basis of the assumption of independent complexation of Ca²⁺ and Mg²⁺ to KCM-1, fluorescence intensity at certain excitation/emission wavelength was calculated as following.

$$\text{fluorescence intensity } (\lambda_{\text{ex}}, \lambda_{\text{em}}) = [I]_0 \{ f_I + f_{\text{ICa}^{2+}} K_{\text{Ca}^{2+}} [\text{Ca}^{2+}] + f_{\text{IMg}^{2+}} K_{\text{Mg}^{2+}} [\text{Mg}^{2+}] \} (1 + K_{\text{Ca}^{2+}} [\text{Ca}^{2+}] + K_{\text{Mg}^{2+}} [\text{Mg}^{2+}])^{-1} \quad (1)$$

where K represents the association constant; I stands for the indicator (fluorescent probe) and ICa^{2+} and IMg^{2+} for the indicator–ion complex; f is a proportionality factor for the individual fluorescent compounds.

Inserting the ratio of the fluorescence intensities at different wavelengths results in eq 1 becoming independent of the initial indicator concentration, and using data obtained from a combination of three different excitation/emission wavelengths, the Ca²⁺ and Mg²⁺ concentrations can be determined. (For further details, refer to the Supporting Information.) A curve fitting based on eq 1 to the experimental data was in good agreement for concentrations lower than 10 μ M Ca²⁺ and 10 mM Mg²⁺ ($R > 0.999$).

At very high Ca²⁺ and Mg²⁺ levels, a slight deviation from the fit according to eq 1 is observed, although such situations are not likely to occur in normal cells. The deviation is assumed to result

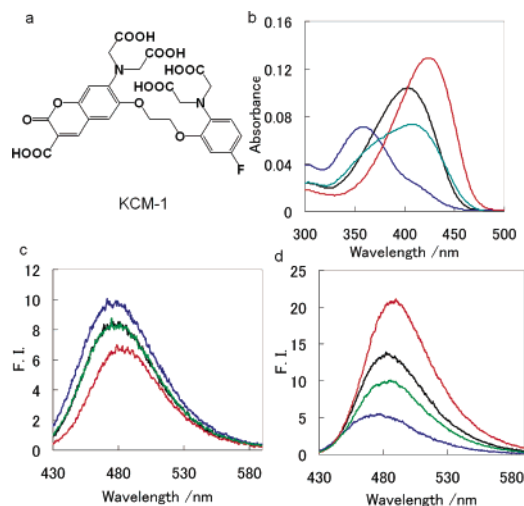


Figure 1. (a) Structure of Ca^{2+} - Mg^{2+} multifluorescent probe KCM-1. (b–d) Absorbance and fluorescence spectra of 10 mM KCM-1 in the absence of Ca^{2+} and Mg^{2+} (black line), in the presence of 1 mM Ca^{2+} (blue line), 500 mM Mg^{2+} (red line), and coexistence of 10 mM Ca^{2+} and 10 mM Mg^{2+} (green line); (b) absorbance, (c) fluorescence (excited at 358 nm), (d) fluorescence (excited at 424 nm). All spectra were measured at pH 7.20 (50 mM HEPES, 130 mM KCl, 20 mM NaCl).

Table 1. Optical Properties and Binding Characteristics of KCM-1^a

compound	λ_{max} nm	ϵ $\text{M}^{-1}\text{cm}^{-1}$	$F\lambda$ nm	K_d
KCM-1	403	10400	480	
KCM-1 (Ca^{2+})	358	7100	475	14 μM
KCM-1 (Mg^{2+})	424	12900	485	26 mM

^a All data were taken in buffer simulating biological conditions (50 mM HEPES, pH 7.2, 130 mM KCl, 20 mM NaCl); ϵ stands for the extinction coefficient, and K_d for the dissociation constants. The probe and cation concentrations during the measurements were 10 μM for KCM-1, 1 mM Ca^{2+} for KCM-1 (Ca^{2+}) and 500 mM Mg^{2+} for KCM-1 (Mg^{2+}).

from the simultaneous complexation of both Ca^{2+} and Mg^{2+} to the same probe molecule. In such a case, the binding of one ion might affect the second binding site and is expected to reduce its affinity toward the cation.

The esterified derivative KCM-1AM was synthesized as an indicator suitable for loading into cells,¹⁶ and KCM-1 was successfully loaded into differentiated PC12 cells. Solving eq 1 for images taken at three different excitation wavelengths (365, 390, 420 nm), we observed that the intracellular concentrations of Ca^{2+} and Mg^{2+} were converted to the image. The mitochondria uncoupler FCCP (carbonyl cyanide *p*-(trifluoromethoxy)phenylhydrazone) was applied to the KCM-1-loaded PC12 cells in order to evaluate the intracellular Ca^{2+} and Mg^{2+} dynamics by imaging with KCM-1 (Figure 2). With administration of FCCP, the intracellular Ca^{2+} concentration was immediately increased and accompanied by a slower Mg^{2+} increase. This observation is consistent with a previous report stating that the mitochondria act as Ca^{2+} and Mg^{2+} stores,¹⁰ and their different kinetics imply their independent transport mechanism across the mitochondrial membrane.

We successfully applied the single-molecular multianalyte sensor KCM-1 for the simultaneous imaging of intracellular Ca^{2+} and Mg^{2+} due to the different optical response patterns of the two selective binding sites.

Using KCM-1 will allow the correlation of intracellular Ca^{2+} and Mg^{2+} to be clarified. Also, applying a high-power microscope,

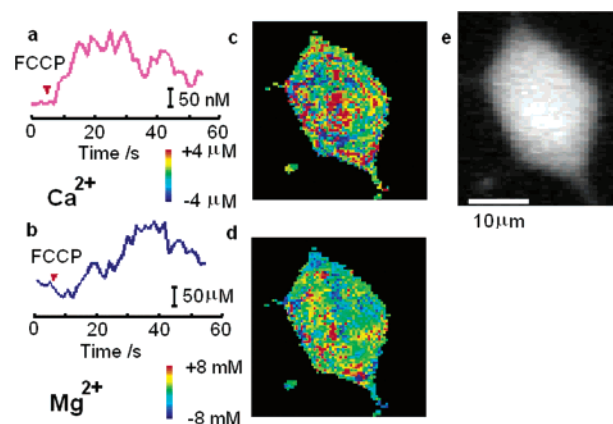


Figure 2. FCCP responses of Ca^{2+} and Mg^{2+} in cytosol of a PC12 cell loaded with KCM-1AM; time course of concentrations of Ca^{2+} (a) and Mg^{2+} (b) in cytosol, fluorescent image of Ca^{2+} change (c, between 0 and 21 s) and of Mg^{2+} change (d, between 0 and 38 s). FCCP was applied at 5 s. Fluorescent image of the PC12 cell excited at 420 nm (e).

the measurement of the intracellular local concentrations will become possible. This is the first reported example of the simultaneous determination of multiple analytes in a cell with a single-molecular multianalyte sensor. Soon, observations of multiple signal transmitter dynamics are going to clarify the central problems in cellular biology.

Supporting Information Available: Experimental details. This material is available free of charge via the Internet at <http://pubs.acs.org>.

References

- Haugland, R. P. *Handbook of Fluorescent Probes and Research Chemicals*, 9th ed.; Molecular Probes: Eugene, OR, 2002.
- Grynkiwicz, G.; Poenie, M.; Tsien, R. Y. *J. Biol. Chem.* **1985**, *260*, 3440–3450.
- Minta, A.; Kao, J. P. Y.; Tsien, R. Y. *J. Biol. Chem.* **1989**, *264*, 8171–8178.
- Suzuki, Y.; Komatsu, H.; Ikeda, T.; Saito, N.; Araki, S.; Citterio, D.; Hisamoto, H.; Kitamura, Y.; Kubota, T.; Nakagawa, J.; Oka, K.; Suzuki, K. *Anal. Chem.* **2002**, *74*, 1423–1428.
- Komatsu, H.; Iwasawa, N.; Citterio, D.; Suzuki, Y.; Kubota, T.; Tokuno, K.; Kitamura, Y.; Oka, K.; Suzuki, K. *J. Am. Chem. Soc.* **2004**, *126*, 16353–16360.
- Nagano, T.; Yoshimura, T. *Chem. Rev.* **2002**, *102*, 1235–1269.
- (a) Miyata, H.; Hayashi, H.; Suzuki, S.; Noda, N.; Kobayashi, A.; Fujiwake, H.; Hirano, M.; Yamazaki, N. *Biochem. Biophys. Res. Commun.* **1989**, *163*, 500–505. (b) Sawano, A.; Hama, H.; Saito, N.; Miyawaki, A. *Biophys. J.* **2002**, *82*, 1076–1085.
- (a) Clapham, D. E. *Cell* **1995**, *80*, 259–268. (b) Carafoli, E. *Proc. Natl. Acad. Sci. U.S.A.* **2002**, *99*, 1115–1122.
- (a) Wolf, F. I.; Torsello, A.; Fasanella, A.; Cittadini, A. *Mol. Aspects Med.* **2003**, *24*, 11–25. (b) Saris, N. E. L.; Mervaala, E.; Karppanen, H.; Khawaja, J. A.; Lewenstam, A. *Clin. Chem. Acta* **2000**, *294*, 1–26.
- Kubota, T.; Shindo, Y.; Tokuno, K.; Komatsu, H.; Ogawa, H.; Kudo, S.; Kitamura, Y.; Suzuki, K.; Oka, K. *BBA-Mol. Cell Res.* **2005**, *1744*, 19–28.
- (a) Mooren, F. C.; Turi, S.; Gunzel, D.; Schlu, W. R.; Domschke, W.; Singh, J.; Lerch, M. M. *FASEB J.* **2001**, *15*, 659–671. (b) Launikonis, B. S.; Stephenson, D. G. *J. Physiol.* **2000**, *526.2*, 299–312.
- Tsien, R. Y. *Biochemistry* **1980**, *19*, 2396–2404.
- (a) London, R. E.; Rhee, C. K.; Murphy, E.; Gabel, S.; Levy, L. A. *Am. J. Physiol.* **1994**, *266*, C1313–C1322. (b) Gee, K. R.; Archer, E. A.; Lapham, L. A.; Leonard, M. E.; Zhou, Z. L.; Bingham, J.; Diwu, Z. *Bioorg. Med. Chem. Lett.* **2000**, *10*, 1515–1518.
- (a) de Silva, A. P.; Gunaratne, H. Q. N.; Gunnlaugsson, T.; Huxley, A. J. M.; McCoy, C. P.; Rademacher, J. T.; Rice, T. E. *Chem. Rev.* **1997**, *97*, 1515–1566. (b) de Silva, A. P.; McClenaghan, N. D. *Chem.—Eur. J.* **2002**, *8*, 4935–4945.
- Regehr, W. G.; Atluri, P. P. *Biophys. J.* **1995**, *68*, 2156–2170.
- Tsien, R. Y. *Nature* **1981**, *290*, 527–528.

JA0528228